SCANNING VOL. 27, 15–22 (2005)

Received: October 14, 2004
Accepted November 30, 2004

"Derived Spectra" Software Tools for Detecting Spatial and Spectral Features in Spectrum Images

DALE E. NEWBURY AND DAVID S. BRIGHT

National Institute of Standards and Technology, Gaithersburg, Maryland, USA

Summary: A spectrum image is recorded as an x-y array of beam locations at each of which a spectrum of radiation is recorded as stimulated by the beam. The large database or "datacube" that results from a single image presents a significant challenge to the analyst to recover information efficiently, especially in the case where a true unknown is examined. This paper describes a class of "derived spectra" software tools that can aid the analyst in recognizing both common and rare features within the datacube. A derived spectrum tool creates a spectrum-like display (intensity vs. channel number) in which the intensity (e.g., x-ray counts) at a particular channel (e.g., x-ray photon energy) is calculated from all of or a subset of the pixel intensities measured for that channel. Derived spectra tools considered include the SUM, MAXIMUM PIXEL, RUNNING SUM, and RUNNING MAXIMUM. The SUM-derived spectrum is useful for recognizing common features of the datacube, while the MAXIMUM PIXEL-and RUNNING MAXIMUM-derived spectra can locate rare, unanticipated features, which may occur as infrequently as being present at a single pixel in the original datacube.

Key words: datacube, derived spectrum, microbeam analysis, scanned probe imaging, spectrum image, x-ray mapping

PACS: 07.79.-v

Introduction

In spectrum imaging, a focused beam of primary radiation is scanned to a series of discrete x-y locations usually selected so as to form a grid on a specimen. While the primary beam is held stationary at a particular location, a complete spectrum of the secondary radiation generated by the interaction of the primary radiation, or a spectrum of the primary radiation itself after interaction, is measured and stored. For more than a decade, spectrum imaging has been established as an effective method for data collection in electron energy loss spectrometry (EELS) in the analytical electron microscope (AEM) because of the inherently high data rate, often reaching MHz counting rates (Jeanguillaume and Colliex 1989).

X-ray spectrum imaging in the scanning electron microscope (SEM) has become a practical mode of data collection with the development of high-speed digital signal processing for the energy dispersive x-ray spectrometer (EDS), extending useful output count rates into the range 30 to 50 kHz (Mott and Friel 1995). As a result, software tools to collect and analyze spectrum images are now commonly available in commercial EDS software systems. Much higher output count rates, ranging above 100 kHz and extending to 500 kHz and even higher, are now possible because of the recent emergence of the silicon drift detector (SDD) (Struder *et al.* 1998). With such high output count rates, useful x-ray spectrum image data sets (e.g., 128×128 pixels at 10 ms dwell per pixel) can be obtained in <5 min, approaching the time necessary for sensitive backscattered electron imaging in the SEM.

Energy dispersive x-ray spectrometer or SDD x-ray spectrum mapping is very likely to become a dominant operational mode for microstructural characterization in the near future. With such capabilities, the analyst will require software tools to locate and extract information efficiently from very large data structures, 100 Mbytes and larger. This problem is being attacked with different approaches. One powerful method employs multivariate curve resolution as the basis for image processing tools that capture the variance between spectral components (Kotula *et al.* 2003). We are pursuing the approach we describe as "derived spectra." Derived spectra are physically meaningful constructions calculated from the measured spectra that comprise the datacube. Derived spectra can capture both common and rare spatial and spectral features contained within the recorded spectrum image data structure (Bright and Newbury 2004). The derived spectra, which have many of the characteristics of real spectra but accentuate certain features of the

Note: The Siegbahn notation is commonly used in the field of electron beam x-ray spectrometry and will be used in this paper. The IUPAC notation is indicated in parentheses at the first use.

Address for reprints:

Dale E. Newbury
National Institute of Standards and Technology
Gaithersburg, MD 20899-8370, USA
e-mail: dale.newbury@nist.gov

sample, can be examined visually or with commonly used peak-finding tools, both of which must closely involve the user in deciding the significance of results. This paper will describe the initial software tool kit that we have developed, with an emphasis on the types of problems where each tool is most effective. All of the software tools we describe are embedded in LISPIX, a comprehensive image and spectrum processing engine, that is available gratis at www.nist.gov/LISPIX.

Materials and Methods

X-ray spectrum images were captured on an SEM operating with a beam energy of 20 keV and equipped with a conventional semiconductor EDS (Si-EDS). The time constant was chosen to operate at the optimum resolution of 135 eV (full peak width at half peak intensity for MnKα). The beam current and detector solid angle were chosen to maintain the system deadtime below 40% and an output count rate of approximately 3000 c/s. A complete spectrum of 2,048 channels of 10 eV width and 2-byte intensity range was collected at each pixel of the map, which was typically scanned at 256×200 pixels with a dwell time of 1 s per pixel to provide adequate counts in each spectrum (14.2 h total).

A polished section of famatinite, a rock with a complex silicate-copper sulfide microstructure, was chosen to provide a range of analytical problems to challenge the derived spectrum software tools that are the subject of this paper.

Spectrum Image Datacubes

The data structure captured in spectrum imaging is often referred to as a "datacube." As illustrated in Figure 1, a typical x-ray spectrum image datacube consists of an x-y scan (e.g., 256 × 256 pixels) with an EDS spectrum consisting of 2,048 channels, each of 10 eV width, recorded at each pixel. The intensity range per channel is two bytes deep, which permits a maximum count of 65,536 in any channel. With the substantially greater output count rates possible with the SDD, it will be necessary to extend the intensity range to at least three and possibly four bytes to avoid losing data due to peak saturation.

The datacube can be considered from two different points of view: (1) a series of x-y data planes, each of which is an x-ray image; examples corresponding to an x-ray peak and the x-ray continuum at a particular channel are shown in Figure 1; and (2) an array of individual EDS x-ray spectra, illustrated in Figure 2. Each spectrum in the array is a conventional x-ray spectrum that is exactly equivalent to the x-ray spectrum that would be recorded in normal operation by placing the beam at the particular location on the specimen for the same dose (beam current x live-time) used for spectrum imaging. Consequently, these individual pixel x-ray spectra have all the features (characteristic peaks and continuum background) and artifacts (e.g., peak broadening, incomplete charge distortions, coincidence peaks, escape peaks) encountered in conventionally performed EDS spectrometry.

Extracting Information from the Datacube

Several strategies can be employed to interrogate the contents of the datacube. We are generally interested in discovering what elements are represented in the area sampled by spectrum imaging, and what spatial distribution relationships exist among the constituents. For this discussion, a general but arbitrary scale of constituent concentration levels, C, can be described as:

Major: $C > 0.1$ mass fraction (> 10 weight percent)
Minor: $0.01 \leq C \leq 0.1$ (1 weight percent to 10 weight percent)
Trace: $C < 0.01$ (< 1 weight percent)

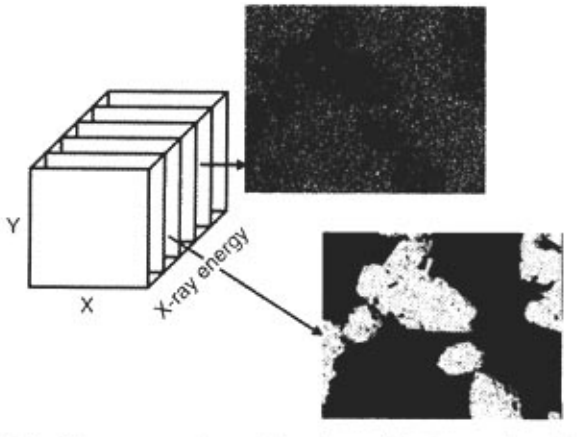

FIG. 1 X-ray spectrum image datacube considered as a series of photon energy planes.

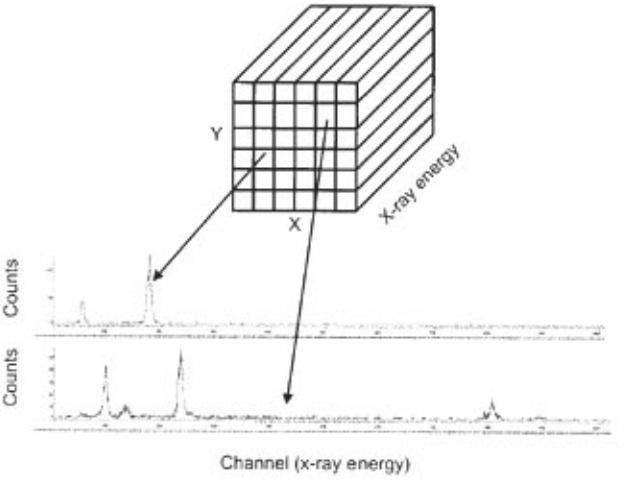

FIG. 2 X-ray spectrum image datacube considered as an array of individual x-ray spectra recorded at each pixel.

"Movie mode" Data Review

A simple "brute force" approach to discover the elemental constituents is to step systematically through the succession of individual image planes as a function of increasing channel number (x-ray energy). This operation can be performed as a continuous sequence and presented to the viewer as a "movie," with an adjustable rate of frame (channel) advance, to make use of the inherent pattern recognition capabilities of the human vision process to detect spatial features of interest. This "movie mode" is often a useful procedure to obtain a general overview of the spectrum image data, especially when a completely unknown and unfamiliar data set is being examined for the first time. "Movie mode" is most useful for detection of prominent features within the datacube, but usually it is not an effective tool for recognizing dilute constituents, detecting rare events, or discovering relationships among constituents.

"Derived Spectrum" Software Tools

We have been investigating a class of software tools for spectrum image operations that we have designated "derived spectrum tools" (Bright and Newbury 2004). A derived spectrum tool creates a spectrum-like display (intensity vs. channel number) in which the intensity at a particular channel (e.g., x-ray photon energy) is calculated from all of or a subset of the intensities measured at the x-y locations for that channel. We do not claim to have originated this class of software tools, at least one of which, the SUMMATION SPECTRUM (usually referred to as the SUM SPECTRUM), described in detail below, has been implemented from the beginning of spectrum imaging (e.g., Gorlen *et al.* 1984, Jeanguillaume and Colliex 1989). The SUM SPECTRUM has been available in commercial AEM/EELS spectrum imaging systems for at least 10 years, and is now commonly implemented in commercial x-ray spectrum imaging systems. Rather, the SUM SPECTRUM is just one member of a broad class of derived spectrum software tools based on various algorithms. Taking the SUM SPECTRUM as a starting point, we are systematically investigating other members of this broad class of tools to determine their specific applicability to certain types of problems.

Sum Spectrum—Detecting Major Spectral Signatures

The SUM SPECTRUM is calculated by sequentially stepping through all of the pixels in a particular x-y plane of the datacube (i.e., a single energy channel) and adding the counts to determine the channel total, as illustrated schematically in Figure 3a. This total becomes the intensity assigned to the corresponding channel in the SUM SPECTRUM:

$$I_{sum}(E) = \sum_x \sum_y I(x, y, E) \quad (1)$$

Figure 3b shows an actual SUM SPECTRUM calculated from an x-ray spectrum image (conditions: 256×200 pixels; conventional EDS operating at a resolution of 135 eV at MnKα) of famatinite, a complex sulfide-silicate rock. The general features of this SUM SPECTRUM correspond closely to those of a real spectrum: (1) peak structures showing the relative intensities expected from the family weights-of-lines, and (2) the continuum background with a shape appropriate to the incident beam energy and a specimen in the form of a flat, bulk target. Using the peaks recognized in the SUM SPECTRUM, we can examine single channel images that correspond to the peak channel or we can add together several adjacent channels that span a peak to obtain better signal-to-noise, as illustrated in Figure 4. Several of the prominent x-ray peaks in Figure 3b were chosen to construct x-ray maps for CuKα ($K\text{-}L_{2,3}$), Figure 4a; SiKα,β, ($K\text{-}M_{2,3}$) Figure 4b; AsLα,β ($L_3\text{-}M_{4,5}$) Figure 4c; and S Kα,β, Figure 4d. Spatial correlations among these constituents for phase analysis can be determined by overlaying the individual maps with color superposition methods in which each constituent is assigned to a primary color, so that the appearance of secondary colors indicates pixel coincidence.

Recognizing Phases: The MASKED SUM SPECTRUM Tool

The intensity level recorded at a pixel for a particular constituent is related to the composition at that x-y location. An x-ray map for a particular constituent is constructed by first choosing the desired channel or range of channels from the SUM SPECTRUM. The x-y image corresponding to a single channel can be viewed directly. If a range of contiguous channels is chosen, such as those that

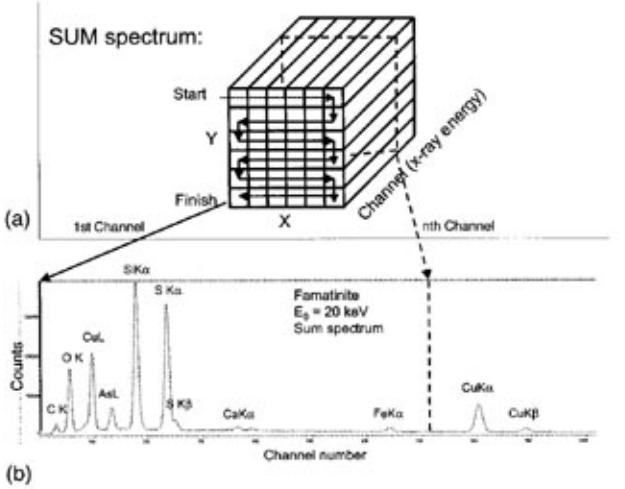

FIG. 3 (a) Calculation sequence for the SUM SPECTRUM; (b) SUM SPECTRUM from an x-ray spectrum image of famatinite, a complex silicate-sulfide rock.

span a peak in the SUM SPECTRUM, then the intensities for all channels are added to find the total for each pixel to create the SUM IMAGE, examples of which are shown in Figure 4.

Since the intensity is related to composition, it may be possible to recognize different intensity levels within the SUM IMAGE, which correspond to different compositions or phases, as is the case for the S Kα,β x-ray map in Figure 4d. The S Kα,β x-ray map can be seen to contain two distinct intensity levels, which can be separated by means of a thresholding tool in LISPIX, producing the masks shown in Figure 5a and c. These masks can be used to determine the MASKED SUM SPECTRUM, shown in Figure 5b and d, in which only the pixels defined by the masked area are included in the summing process to determine the x-ray spectrum of each phase. The MASKED SUM SPECTRUM tool reveals the presence of the phases FeS_2 (pyrite) and CuS (cuprite). The CuS spectrum further reveals that arsenic is segregated to the CuS phase, which can also be confirmed by superimposing the Cu and AsL x-ray maps. Since the number of pixels and the deadtime-adjusted dwell time are known, these MASKED SUM SPECTRA could be used in a standards-based quantitative analysis procedure. Similar tools are often incorporated in commercial software packages for spectrum imaging.

Minor Intensity Features

By expanding the intensity axis of the SUM SPECTRUM, either linearly or logarithmically, intensities corresponding to minor level components become visible, as shown in Figure 6a for detection of FeKα–Kβ, and the corresponding FeKα map in Figure 6b. Locally, the iron is a major constituent of the FeS_2 phase, but because this phase occurs in only a small percentage of the map pixels, the Fe appears as a minor peak in the SUM SPECTRUM. As a phase becomes rarer as a spatial fraction, the SUM SPECTRUM by its nature tends to suppress the visibility of the particular spectral features of that rare phase because the statistics of the intensity at any channel in the SUM SPECTRUM are determined by the spatially dominant phases.

MAXIMUM PIXEL SPECTRUM: Detecting Rare, Unanticipated Features

As shown in Figure 7a, the MAXIMUM PIXEL SPECTRUM (Bright and Newbury 2004) is calculated in a fashion similar to the SUM SPECTRUM, except that the algorithm finds the maximum value of the intensity represented at any pixel location within an x-y image plane (channel). This maximum value is then placed in that particular en-

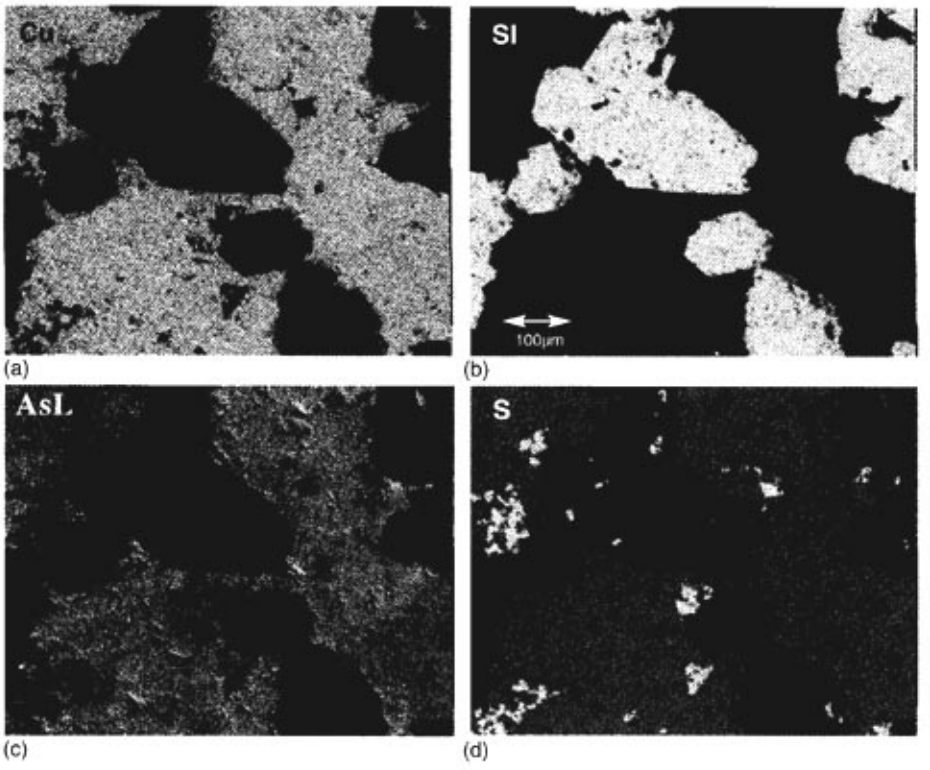

FIG. 4 Elemental distribution maps recovered from the SUM SPECTRUM of Figure 3b by integrating the characteristic peaks and plotting the integrated intensity at each pixel: (a) CuKα, (b) SiK, (c) AsL, and (d) S Kα,β.

ergy channel to construct the MAXIMUM PIXEL derived spectrum:

$$I_{max}(E) = \max\left[I(x,y,E)\right] \quad (2)$$

The MAXIMUM PIXEL SPECTRUM has been found to be sensitive to rare, unanticipated spectral features even if a feature only occurs at a single pixel. As long as the rare phase has a spectral characteristic, for example, a unique peak, it will be detectable with the MAXIMUM PIXEL SPECTRUM. Because the statistics of the MAXIMUM PIXEL SPECTRUM are restricted by its very definition to the statistics of a single pixel, a rare event, even one that occurs at only a single pixel, is given equal weight in constructing the MAXIMUM PIXEL SPECTRUM with the much more dominant features. Despite their high spatial frequency, dominant features of the spectrum image are also represented by single pixel statistics in the MAXIMUM PIXEL SPECTRUM, whereas in the SUM SPECTRUM the statistics represent the total counts recorded at every channel.

The MAXIMUM PIXEL SPECTRUM obtained from the famatinite spectrum image is shown in Figure 7b and is overlaid with the SUM SPECTRUM in Figure 8. Comparison of these spectra reveals at least three significant peaks in the MAXIMUM PIXEL SPECTRUM that are absent from the SUM SPECTRUM, labeled "1," "2," and "3:"

Peak "1" corresponds to AlKα, and the x-ray map recovered from this peak consists of a single pixel, shown (within the circle) in Figure 9a. The spectrum recovered from the spectrum image for this pixel is shown in Figure 9b, which reveals AlK and O K, probably from a single particle of the Al_2O_3 remaining as a contaminant after alumina was used to polish the specimen.

Peak "2" corresponds to ClKα, and Figure 10a shows the image from this peak, which contains two separate one-pixel objects. The resulting MASKED SUM SPECTRUM for these pixels, Figure 10b, shows major peaks for NaKα and ClKα, probably arising from NaCl contaminants.

Finally, peak "3" has the energy of K Kα, and the x-ray map recovered from this peak, shown in Figure 11a, shows several well dispersed single pixels and small pixel arrays. When the MASKED SUM SPECTRUM is determined for these objects, Figure 11b, it can be seen that the SnL family of peaks is found rather than K Kα and K Kβ, demonstrating the need for a careful study of all the information available before reaching conclusions. This spectrum also

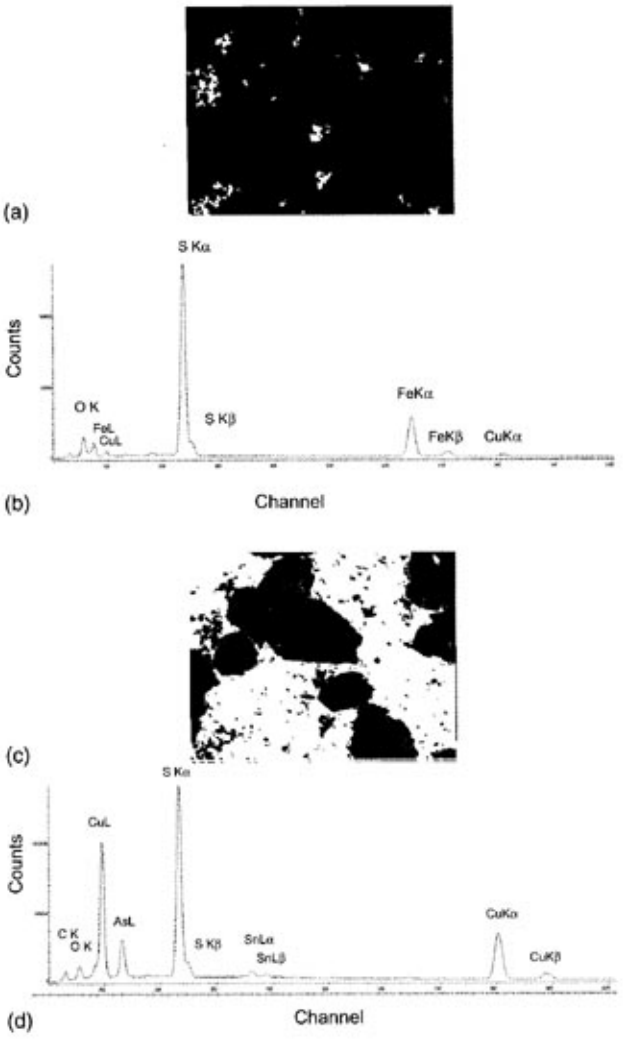

FIG. 5 (a) Sulfur elemental mask obtained by selecting the higher intensity features in Figure 4d; (b) x-ray spectrum summed from pixels in this mask showing iron sulfide; (c) Sulfur elemental mask obtained by selecting the lower intensity features in Figure 4d; (d) x-ray spectrum summed from pixels in this mask showing copper sulfide.

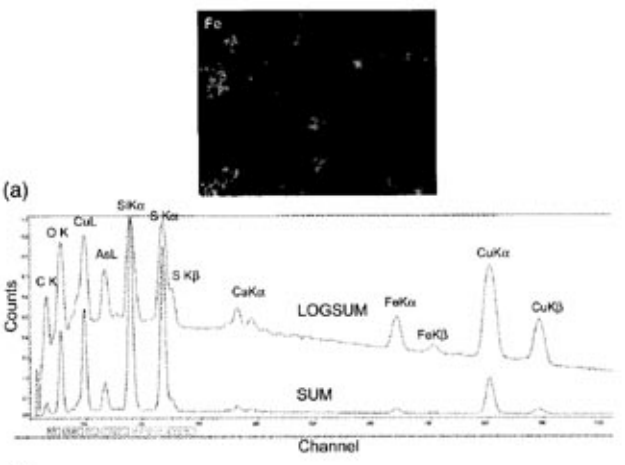

FIG. 6 (a) Use of logarithm to enhance vertical sensitivity in presenting SUM SPECTRUM data for the famatinite x-ray spectrum image. (b) X-ray map for iron recovered by selecting the FeKα peak in Figure 6a.

contains significant sulfur, suggesting that the tin component is present as discrete inclusions in the copper sulfide phase, rather than a contaminant.

Sequential algorithms

Mathematical operations can be performed sequentially to construct derived spectra. For example, consider a single smoothing operation, in which an arithmetic mean filter is passed through the SUM SPECTRUM. This filter operation determines the mean for a given channel n by averaging it with m channels below and above the channel being determined:

$$I_{RUNNING\_SUM}(E)_n = \frac{\sum_{i=n-m}^{i=n+m} I(E)_i}{2m+1} \quad (3)$$

This procedure produces the RUNNING SUM SPECTRUM. The RUNNING SUM SPECTRUM for the famatinite spectrum image is shown superimposed on the SUM SPECTRUM in Figure 12. No additional peaks are recognized in the RUNNING SUM SPECTRUM compared with the SUM SPECTRUM. The only effect observed is

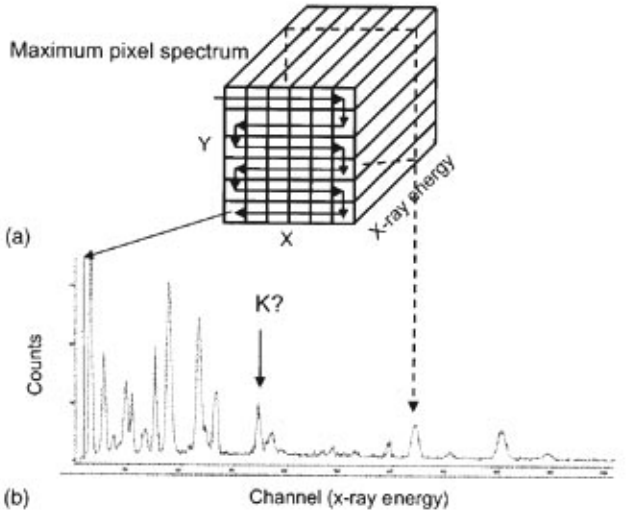

FIG. 7 (a) Calculation sequence for the MAXIMUM PIXEL SPECTRUM; (b) MAXIMUM PIXEL SPECTRUM from the same x-ray spectrum image of famatinite used for the SUM SPECTRUM in Figure 3.

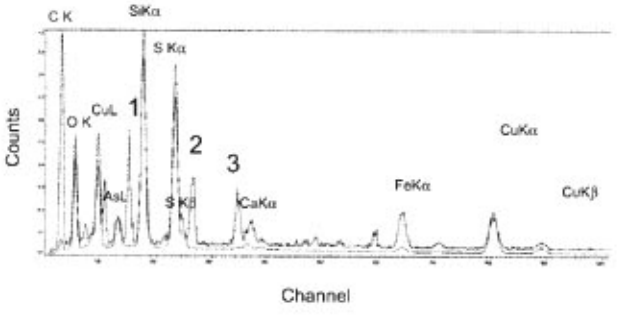

FIG. 8 Overlay of the SUM SPECTRUM and the MAXIMUM PIXEL SPECTRUM from the x-ray spectrum image of famatinite. Numbers indicate prominent peaks recognized in the MAXIMUM PIXEL SPECTRUM that are not obvious in the SUM SPECTRUM.

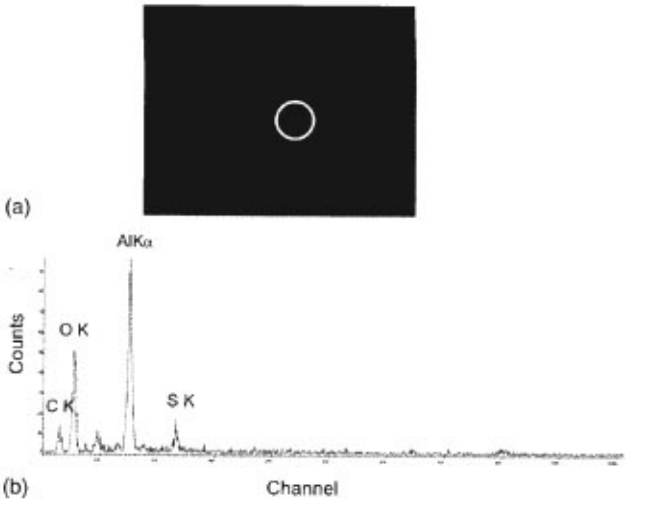

FIG. 9 (a) X-ray map for Al created from the "1" peak in Figure 8 revealing a single pixel (within circle); (b) single pixel spectrum corresponding to the pixel highlighted in Figure 9a.

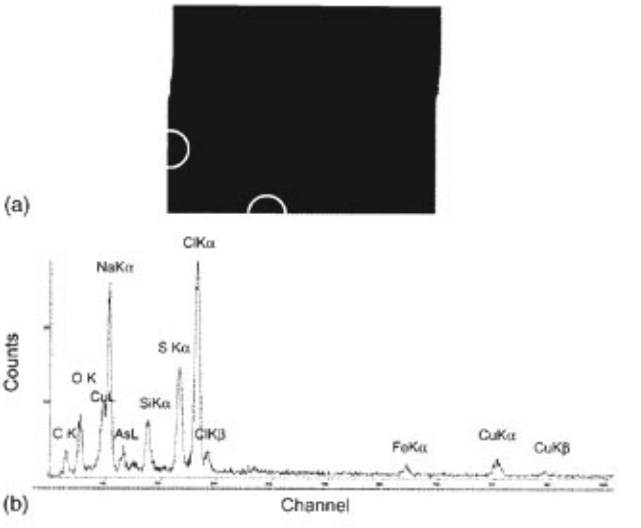

FIG. 10 (a) X-ray map for Cl created from the "2" peak in Figure 8 revealing two pixels (within circles); (b) MASKED SUM SPECTRUM corresponding to the two pixels highlighted in a. Note Cl Kα and Cl Kβ.

the expected slight degradation of resolution that is inevitable in a smoothing operation, best recognized in Figure 12 by the loss of the distinct S Kβ peak from the RUNNING SUM SPECTRUM.

However, a useful sequential operation can be performed by first applying the smoothing operation of Eq. (3) to each pixel spectrum (i.e., smoothing the entire spectrum image) followed by determining the maximum pixel value taken from each x-y plane of the smoothed spectrum image. This sequence of operations results in a newly derived spectrum, the RUNNING MAXIMUM SPECTRUM (shortened to "RUNNING MAX"). The MAXIMUM PIXEL SPECTRUM and the RUNNING MAX SPECTRUM are overlaid in Figure 13. While most peaks are identical in these two spectra, there are two additional peaks observed in the RUNNING MAX SPECTRUM, labeled "1" and "2." While these features may be considered to be at the threshold of visibility in the original MAXIMUM PIXEL SPECTRUM, they could easily have been dismissed as mere statistical noise.

Peak "1" is found to correspond to MnKα, and the resulting image constructed from this peak reveals a single pixel, Figure 14a. The corresponding pixel spectrum, Figure 14b, confirms the MnKα-MnKβ identification and further reveals associated sulfur, so that it is likely that this is a MnS inclusion, rather than a contaminant.

Peak "2" is found to correspond to CeLα, and the x-ray map constructed from this peak shows two separated single-pixel particles, Figure 15a. The MASKED SUM SPECTRUM from these two pixels, Figure 15b, shows a

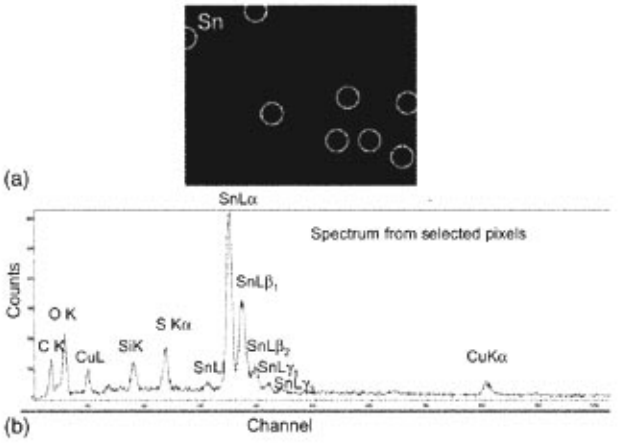

FIG. 11 (a) X-ray map for created from the "2" peak in Figure 8 revealing several pixels (within circles); (b) MASKED SUM SPECTRUM corresponding to the pixels highlighted in Figure 11a. Note that the "2" peak arises from the SnL family and not K Kα-Kβ.

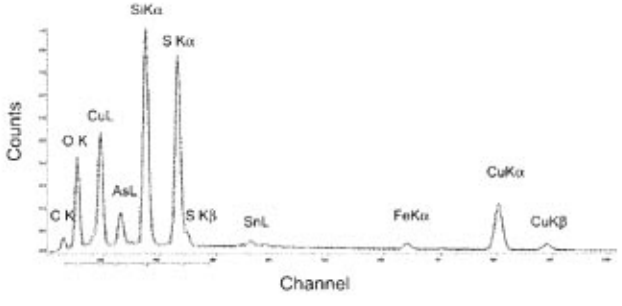

FIG. 12 Overlay of the RUNNING SUM SPECTRUM and the SUM SPECTRUM from the x-ray spectrum image of famatinite. No new information is retrieved from the RUNNING SUM SPECTRUM in this example.

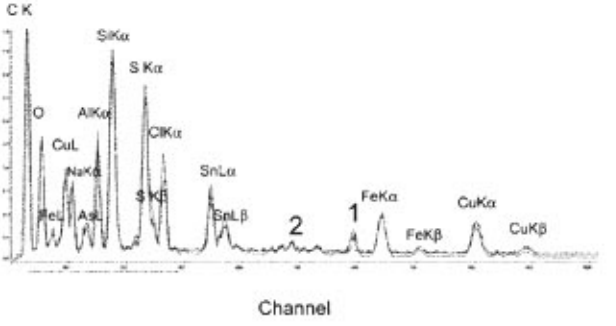

FIG. 13 Overlay of the RUNNING MAX SPECTRUM and the MAXIMUM PIXEL SPECTRUM from the x-ray spectrum image of famatinite. Two features, labeled "1" and "2," become more easily detected as peak structures in the RUNNING MAX SPECTRUM.

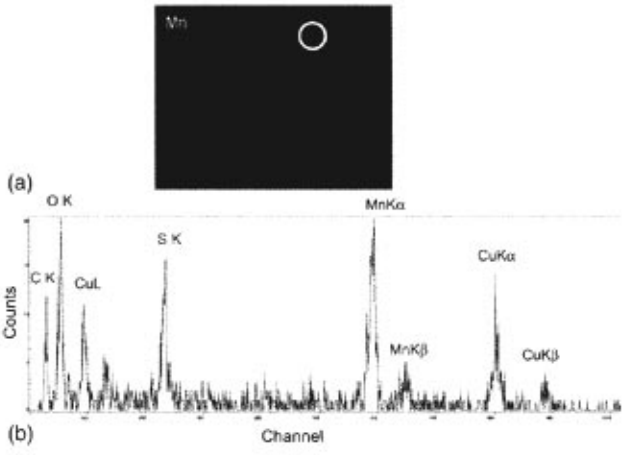

FIG. 14 (a) X-ray map created from the "1" peak in the RUNNING MAX SPECTRUM of Figure 13, revealing a single pixel (within circle); (b) single-pixel spectrum corresponding to the pixel highlighted in Figure 14a. Note the Mn Kα and Mn Kβ peaks, as well as S K, suggesting a MnS phase as an inclusion in the CuS matrix.

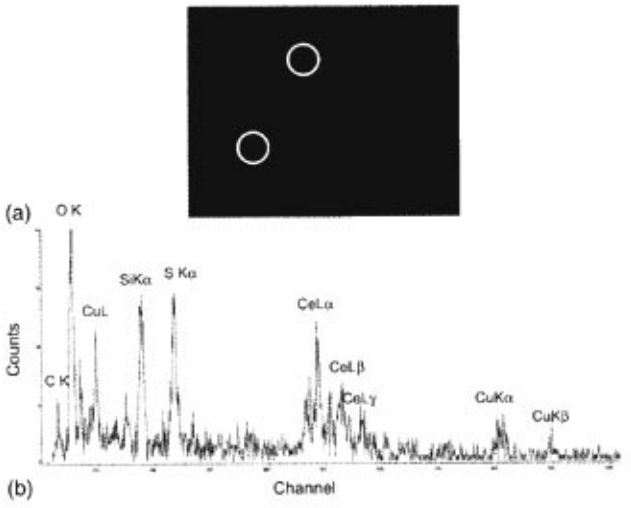

FIG. 15 (a) X-ray map created from the "2" peak in the RUNNING MAX SPECTRUM of Figure 13, revealing two pixels (within circles); (b) two-pixel MASKED SUM SPECTRUM corresponding to the pixels highlighted in Figure 15a: Note the CeLα-CeLβ-CeLγ sequence.

complex spectrum which has the expected relative intensity sequence for CeLα-CeLβ-CeLγ. Observing this intensity sequence is a strong indicator for the Ce identification, despite the low number of counts available. Clearly, this identification is very near the threshold of detection and great care must be taken to avoid false positives.

These examples demonstrate the utility of the RUNNING MAX SPECTRUM to recover information down to the noise threshold. However, the examples also indicate the need for checking the original spectral data carefully to make a robust determination of the significance of any low level features in derived spectra, especially those that involve a smoothing operation. It is critical that the derived spectra only be used as guides to identify possible spectral features of interest followed by careful inspection of the true pixel spectra, either individually or grouped, using the MASKED SUM SPECTRUM.

Conclusions

Derived spectrum software tools provide a flexible and powerful approach to the problem of recovering information from spectrum image data cubes. Derived spectrum software tools can recover major and minor features, distinguish phases separated by small changes in composition, and recover rare, unanticipated features, down to features that occur at the single pixel level. The variety of possible derived spectrum tools is not yet fully explored, and it is likely that additional tools will be discovered based upon other calculation algorithms, including sequence processing involving two or more steps.

References

Bright DS and Newbury DE: Maximum pixel spectrum: A new tool For detecting And recovering rare, unanticipated features from spectrum image data cubes. *J Microsc* 216, 186–193 (2004)

Gorlen KE, Barden LK, Del Priore JS, Fiori CE, Gibson CC, Leapman RD: Computerized analytical electron microscope for elemental imaging. *Rev Sci Instrum* 55, 912–921 (1984)

Jeanguillaume C, Colliex C: Spectrum image: the next step in EELS digital acquisition and processing. *Ultramicroscopy* 28, 252–257 (1989)

Kotula P, Keenan MR, Michael Jr. JR: Automated analysis of SEM x-ray spectralimages: A powerful new microanalysis tool. *Microsc Microanal* 9, 1–17 (2003)

Mott RB, Friel JJ: Improving EDS performance with digital pulse processing. In *X-ray Spectrometry in Electron Beam Instruments* (Eds. Williams DB, Goldstein JI, Newbury DE). Plenum, New York (1995) 127–157

Struder L, Fiorini C, Gatti E, Hartmann R, Holl P, Krause N, Lechner P, Longoni A, Lutz G, Kemmer J, Meidinger N, Popp M, Soltau H, von Zanthier C: High resolution non-dispersive x-ray spectroscopy with state of the art silicon detectors. *Mikrochim Acta* 15 (1998) (suppl): S11-S19